

Marcin KARGUL*, Joanna BOROWIECKA-JAMROZEK*, Marek KONIECZNY*

THE EFFECT OF THE ADDITION OF ZEOLITE PARTICLES ON THE PERFORMANCE CHARACTERISTICS OF SINTERED COPPER MATRIX COMPOSITES

WPLYW DODATKU CZĄSTEK ZEOLITU NA WŁAŚCIWOŚCI EKSPLOATACYJNE SPIEKANEGO KOMPOZYTU O OSNOWIE MIEDZI

Key words:

sinter, copper, zeolite, metal matrix composite, wear resistance.

Abstract

The paper presents the results of research on the possibilities of producing and using copper–zeolite composites obtained by powder metallurgy. The zeolite powder (0.0–0.2 mm fraction) used in the experiments was ground tuff rock extracted from the Kucin Quarry (VSK PRO-ZEO s.r.o.) in Slovakia. The as-delivered material was imaged and analysed using the SEM/EDS and XRD techniques. Before the sintering process, one-sided pressing was applied to the hydraulic press at a pressure of 620 MPa. The sintering process was carried out in a laboratory tube furnace at 900°C in an atmosphere of dissociated ammonia. The sintering time was 60 minutes. The resulting agglomerates were subjected to the following tests: measurements of density, hardness, electrical conductivity, and abrasion resistance. Observations of the microstructure on metallographic specimens made from the sintered samples were also performed using a scanning electron microscope (SEM). Zeolite was introduced into the copper matrix in the amounts of 2.5, 5, 7.5, and 10% by weight. The introduction of zeolite particles into the matrix as the strengthening phase caused an increase in the hardness of sinters while lowering a density and electrical conductivity. The introduction of zeolite particles caused a decrease in abrasion resistance for a composite containing up to 7.5% zeolite. The increase in abrasion resistance was observed for the composite containing 10% zeolite particles.

Słowa kluczowe:

spiek, miedź, zeolit, kompozyt z metalową osnową, odporność na zużycie ściernie.

Streszczenie

W pracy przedstawiono wyniki badań nad możliwościami wytwarzania i zastosowania kompozytu miedź–zeolit otrzymanego za pomocą technologii metalurgii proszków. Proszek zeolitu (frakcja 0.0–0.2 mm) wykorzystany do badań pozyskano ze skały zwanej tufem zeolitytowym, wydobywanej w kopalni Kucice, (VSK PRO-ZEO s.r.o.), Słowacja. Proszek zeolitu został poddany obserwacjom SEM/EDS oraz rentgenowskiej analizie fazowej XRD. Przed procesem spiekania zastosowano jednostronne prasowanie na prasie hydraulicznej przy ciśnieniu prasowania 620 MPa. Proces spiekania przeprowadzono w laboratoryjnym piecu rurowym w temp 900°C w atmosferze zdysocjowanego amoniaku. Czas spiekania wynosił 60 minut. Wytworzone spieki poddano następującym badaniom: pomiarowi gęstości, twardości, przewodności elektrycznej oraz odporności na zużycie ściernie. Przeprowadzono również obserwacje mikroskopowe zglądów metalograficznych wykonanych z badanych spieków z użyciem skaningowego mikroskopu elektronowego (SEM). Zeolit wprowadzono do miedzianej osnowy w ilościach 2,5, 5, 7,5, 10% wagowych. Wprowadzenie do osnowy cząstek zeolitu jako fazy umacniającej spowodowało podwyższenie twardości spieków, natomiast obniżenie gęstości i przewodności elektrycznej. Wprowadzenie cząstek zeolitu w ilości do 7,5% spowodowało obniżenie odporności na zużycie ściernie. Wzrost odporności na zużycie ściernie zaobserwowano dla kompozytu zawierającego 10% zeolitu.

INTRODUCTION

Over the past few decades, the development of metal-ceramic composite sinters for structural elements with increased mechanical strength and abrasion resistance

has been observed. The use of this technology allows one to eliminate problems found in the casting technique, which are related to the poor wettability of ceramic particles by the liquid metal. In addition, when casting, we deal with the heterogeneity of the location of

* Kielce University of Technology, Faculty of Mechatronics and Mechanical Engineering, Department of Metal Science and Materials Technologies, Al. Tysiąclecia P.P. 7, 25-314 Kielce, Poland, e-mails: mkargul@tu.kielce.pl, jamrozek@tu.kielce.pl, mkon@tu.kielce.pl.

the reinforcing phase [L. 1–7]. Among metal composite materials, composites with a copper matrix deserve special attention. The introduction of ceramic particles of the oxide type (Al_2O_3 , ZrO_2 , TiO_2), carbides (SiC , TiC), or graphite for copper alloys allows to the creation of wear-resistant composites with increased strength [L. 8–14]. Reinforcement with ceramic particles also ensures that the working temperature is increased. High resistance to abrasion of composites is ensured by oxides and carbides particles with diameters above $100\ \mu\text{m}$ [L. 15, 16]. For many applications, materials that are resistant to high temperatures and with high thermal conductivity are necessary. For such applications, copper is irreplaceable because it has the highest thermal conductivity among construction materials [L. 17, 18]. The literature review shows that the research of copper-matrix sinters was carried out using volcanic tuff as the reinforcement. Analysing the results of these studies, it can be concluded that the addition of tuff lowered the density and porosity, as well as increased the hardness of the tested sinters [L. 19–22]. Following the aforementioned research, the study presents the possibilities of using zeolite particles as a strengthening phase. Zeolites are a group of natural hydrated aluminosilicates with different chemical composition and properties. The zeolite consists of porous aluminosilicates with an expanded surface containing a number of hard and refractory oxides. These are sodium and calcium aluminosilicates, and to a lesser extent, barium, strontium, potassium, magnesium, and manganese. The properties of aluminosilicates stem from their crystalline structure, which is characterized by the existence in the spatial aluminosilicate skeleton of channels and chambers with strictly defined molecular dimensions. Thanks to unique properties, e.g., the negative charge of crystal lattice, crystalline structure, thermal and hydrothermal stability, the uniform size of micropores, easy exchangeability of non-network cations, and others, they can be used in various fields, such as ion exchange, catalysis, water and exhaust purification, and processing crude oil. An additional advantage is the low price, availability, porosity, through which it is possible to obtain a good connection to the matrix, a specific gravity which contributes to lowering the mass of the composite, as well as the thermal

resistance of the composite that allows the production of composites at high temperatures. However, few studies about the physicochemical properties of this mineral and its applications have been published [L. 23–25].

In this work, a composite with a copper matrix in which zeolite particles were used as the reinforcing phase is presented. The preliminary tests of the properties of the produced composite did not show significant sinter consumption, and the powdered zeolite tuff introduced into the metal matrix increased the hardness of sinters, thanks to which, it can be successfully used as a strengthening material. The tests carried out in the presented work will allow us to assess the suitability of this composite and its application possibilities, e.g., for electric brushes for electric motors, power tools, starters and alternators, and industrial machines. Electric brushes are used to make electrical contact between two (or more) moving parts. Usually the brushes work with a commutator or slip rings. Currently, electric brushes are usually made of graphite and graphite with the addition of copper [L. 26]. The higher content of graphite has a positive effect on the smaller wear of commutators and rings. However, the material with a higher copper content is used at high current densities, in low voltage DC current machines, and with high currents, e.g., car starters. Brushes require constant pressure. As the device is used, brushes are rubbed off, because they are constantly pressed against the place of contact. Therefore there is a need for a flexible connection. As the device is working, regular wear of brushes occurs, which from time to time must be changed with new ones. The conducted tests indicate that the produced sinters will be used in the production of brushes.

MATERIALS AND METHODS

The materials used in the experiment to fabricate the composites were commercial powders. Copper powder (99.5% Cu) with an average particle size of less than $63\ \mu\text{m}$ was used as the matrix, and zeolite, with an average particle size of less than $0.2\ \text{mm}$, was used as the reinforcement. The shapes and arrangements of the powder particles used in the experiments are shown in **Figure 1**.

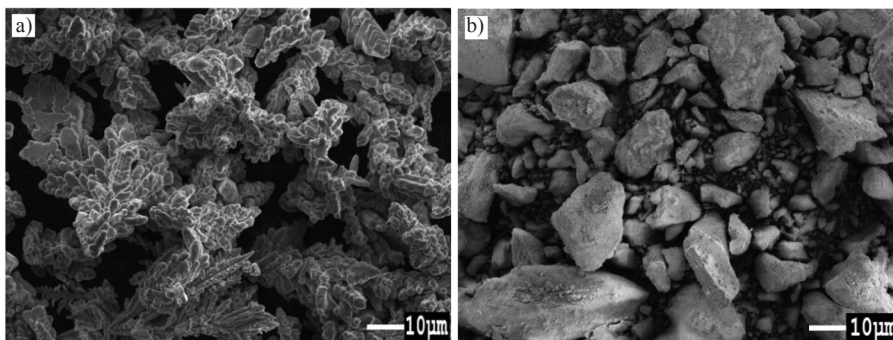


Fig. 1. Images of the tested powders: a) electrolytic copper powder, b) zeolite powder
Rys. 1. Zdjęcia badanych proszków: a) elektrolityczny proszek miedzi, b) proszek zeolitu

Before the fabrication of composites, the powders were observed using a JEOL JSM-7100F field emission scanning electron microscope fitted with OXFORD INSTRUMENTS EDS X-Max AZtec software for elemental microanalysis.

The surface composition of the as-delivered zeolite particles is illustrated in the X-ray diffraction pattern in **Figure 2** and in **Table 1**.

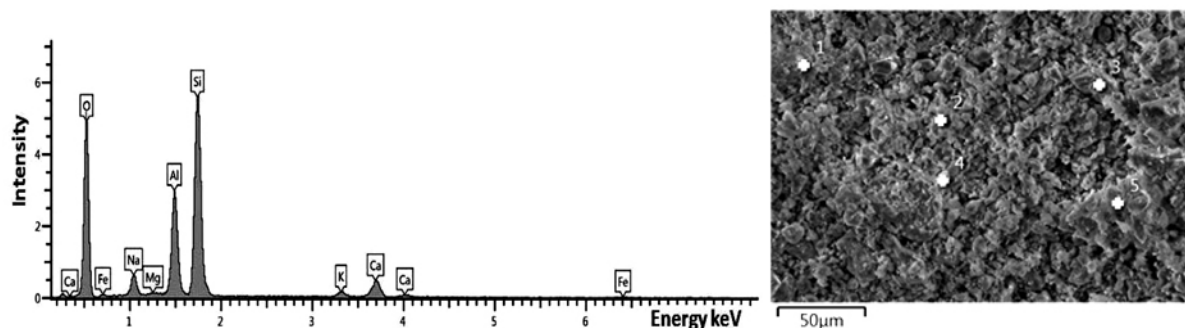


Fig. 2. The energy spectrum for emitted X-rays for as-delivered zeolite particles

Rys. 2. Wynik mikroanalizy rentgenowskiej cząstek zeolitu w stanie dostawy

Table 1. Major elements found in the as-delivered zeolite

Tabela 1. Główne pierwiastki występujące w zeolicie

Al [%]	Si [%]	K [%]	Ca [%]	Fe [%]	Oxygen [%]
5–14	23–32	2–14	1–2.5	0.0–1.5	40–50

Before the consolidation, the as-delivered zeolite material was tested by X-ray diffraction analysis. The phase composition of the zeolite was identified using the powder method, i.e. the Debye-Scherrer-Hull (DSH) method. The analysis was carried out by means of a Bruker D8 Discover diffractometer operating in Bragg-Brentano mode equipped with a $\text{CuK}\alpha$ radiation source, a Ni filter, and a LYNXEYE_XE detector. The mineral composition was determined and calculated on the basis

of the licensed databases by ICDD (International Centre for Diffraction Data), ICSD (Inorganic Crystal Structure Database), and NIST (National Institute of Standards and Technology). The data were registered and analysed using Bruker AXS DIFFRAC v.4.2 and TOPAS v.4.2 software. The phases of the as-delivered zeolite rock samples were identified using X-ray diffraction (XRD) analysis. Phase composition of the as-delivered zeolite is presented in **Table 2**.

Table 2. Phase composition of the as-delivered zeolite

Tabela 2. Skład fazowy zeolitu w stanie dostawy

Phases	Percentage [%]
Clinoptilolite-Ca ((Na, K,Ca)(Al,Si) $\text{Si}_8\text{O}_{18}\cdot 7\text{H}_2\text{O}$)	34–36
Feldspars (potassium feldspar $\text{K}[\text{AlSi}_3\text{O}_8]$ + plagioclase feldspars $\text{Na}[\text{AlSi}_3\text{O}_8]$ (albite) – $\text{Ca}[\text{Al}_2\text{Si}_2\text{O}_8]$ (anorthite) $\text{L2Si}_2\text{O}_8]$ (anortyt)	28–30
Quartz (SiO_2)	11–12
Illite + muskovite ($\text{KAl}_2[\text{AlSi}_3\text{O}_{10}(\text{OH})_2]$)	1–3
Kaolinite ($\text{Al}_4[\text{Si}_4\text{O}_{10}(\text{OH})_8]$)	< 1–2
Amorphous substance	20–21

The crystalline phases obtained by XRD are illustrated in **Figure 3**.

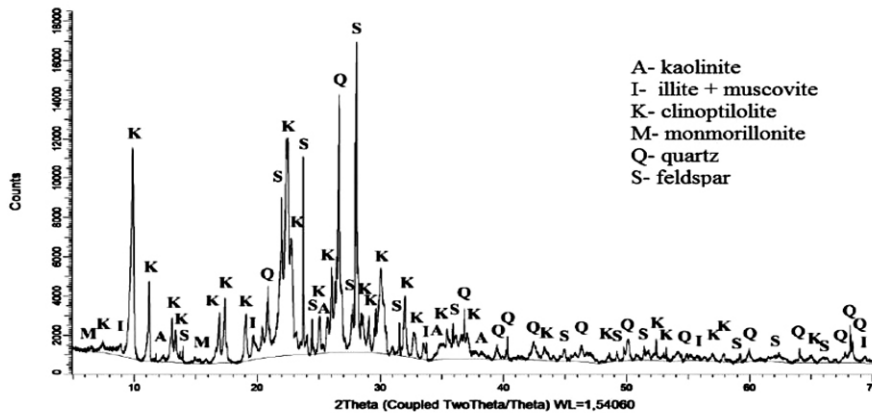


Fig. 3. X-ray diffractogram of the as-delivered zeolite
Rys. 3. Dyfraktogram rentgenowski cząstek zeolitu w stanie dostawy

Before the compaction process, zeolite powders were subjected to calcination process in a furnace at 850° for 60 minutes. The purpose of calcination process was to remove the rest of organic materials and removal the moisture.

The surface composition of the zeolite particles after the calcinations process is illustrated in the X-ray diffraction pattern in **Figure 4** and in **Table 3**.

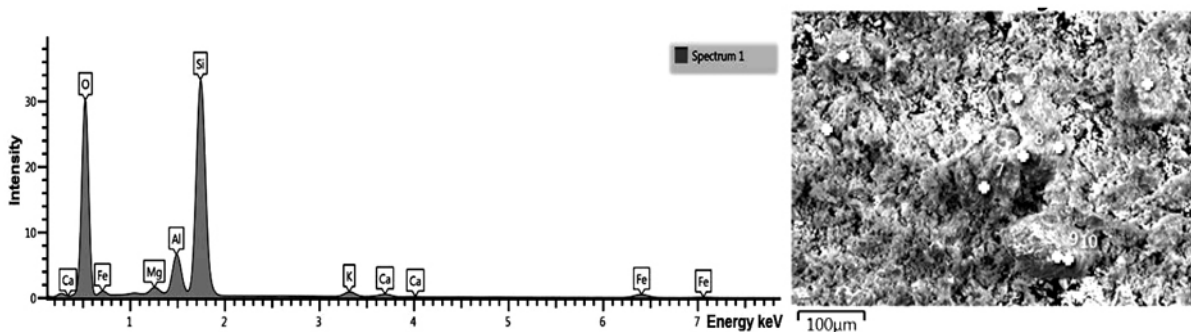


Fig. 4. The energy spectrum for emitted X-rays for zeolite particles after calcinations process
Rys. 4. Wynik mikroanalizy rentgenowskiej cząstek zeolitu po procesie prażenia

Table 3. Major elements found in zeolite after calcinations process

Tabela 3. Główne pierwiastki występujące w zeolicie po procesie prażenia

Al [%]	Si [%]	K [%]	Ca [%]	Fe [%]	Oxygen [%]
1–7	1–36	0.5–2	0.5–2.5	0.5–8	46–95

After the calcination process, the zeolite powders were subjected for further analysis. An X-ray diffraction analysis was performed again to determine the phase composition of the zeolite after heating at a temperature of 850°C. The analysis of the phase composition of the zeolite after heating showed the presence of 43–45% of potassium feldspars, 8–9% of quartz, 5–6% of cristobalite,

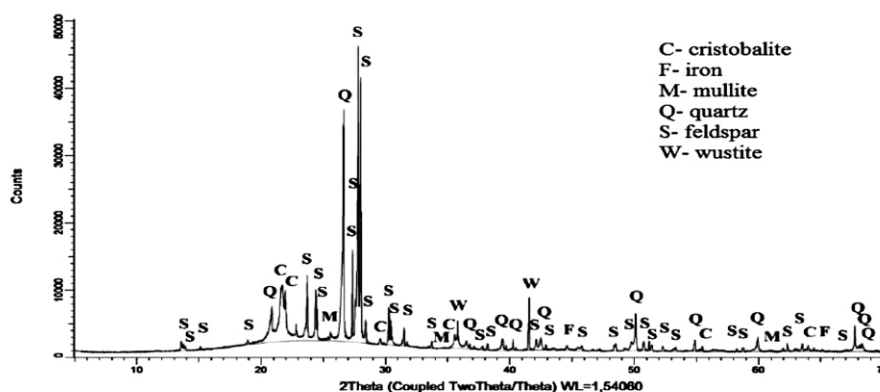
1–2% of mullite, 1–2% of wustite and 39–40% of an amorphous substance. The phases of the zeolite powder after the calcinations process were identified using the X-ray diffraction (XRD) analysis. Phase compositions of the zeolite powder after calcination process are shown in **Table 4**.

Table 4. Phase composition of the zeolite powder after calcination process

Tabela 4. Skład fazowy proszku zeolitu po procesie prażenia

Phases	Percentage [%]
Feldspars (potassium feldspar $K[AlSi_3O_8]$ + plagioclase feldspars $Na[AlSi_3O_8]$ (albite) – $Ca[Al_2Si_2O_8]$ (anorthite) $L2Si_2O_8]$ (anortyt)	43–45
Quartz (SiO_2)	8–9
Cristobalite	5–6
Mullite ($3Al_2O_3 \cdot 2SiO_2$)	<1–2
Wustite (FeO)	< 1–2
Amorphous substance	39–40

The crystalline phases can be seen in the diffractogram in **Figure 5**.

**Fig. 5. X-ray diffractogram of the zeolite after heating at 850°C**

Rys. 5. Dyfraktogram rentgenowski zeolitu po prażeniu w temperaturze 850°C

Powder mixtures with the following content of zeolite, i.e. – 2.5%, 5%, 7.5% and 10% by weight, were prepared for the tests. Finished powdered mixtures were subjected to single-track pressing on a hydraulic press at a compaction pressure of 620 MPa. The specimens with a dimension of $\phi 20 \times 10$ mm were sintered in a silit tubular furnace at 900° for 60 minutes in the dissociated ammonia atmosphere. Finally, the material was cooled in the furnace. After the sintering process, the samples were subjected to the compaction process at a pressure of 620MPa and re-sintering at 900° for 60 minutes. The parameters of the manufacturing processes for sintered composites with zeolite particles are presented in **Table 5**. The sintering parameters were chosen based on previous research and compared with the results available in the literature [L. 20–22]. The sintered compacts were measured for hardness, electrical conductivity, density, and abrasion resistance tests. The hardness of the composites was measured using the Brinell method (with a steel ball 5 mm in diameter at a load of 250 kG) in accordance with the PN EN

ISO 6506-1:2014 standard. The electrical conductivity tests were performed using a GE Phasec 3D device using the eddy current method. The density was determined by weighing the specimens in air and water using WPA120 hydrostatic scales in line with the PN EN ISO 2738:2001 standard. The relative density of the obtained sinters was determined using Formula 1.

$$\rho = \frac{d}{d_i} \cdot 100\% \quad (1)$$

where ρ – relative density, d – true density, d_i – theoretical density.

The abrasion resistance tests of the fabricated composites were conducted using a T-01M ball-on-disc testing machine according to the requirements of the ASTM G 99 standard.

The following parameters were set for the test:

- Friction pair: a 100Cr6 steel ball (10 mm in diameter) and a disc made of copper with a addition of various amount of zeolite (2.5–10% of zeolite);

- Load: $P = 10$ N;
- Sliding velocity: $v = 0,1$ m/s;
- Friction path distance: $s = 1000$ m;
- Humidity: $47 \pm 1\%$;
- Ambient temperature: $T_0 = 25 \pm 1^\circ\text{C}$; and,
- Atmospheric pressure: 987 ± 5 hPa.

The tests were performed under dry friction. The discs were weighed before and after the tests to determine

the loss of weight. Analyses of the geometric structure after the tribological tests were performed using a Talysurf CCI optical profilometer. Microstructure analyses on the metallographic specimens were conducted using a JEOL JSM-7100F field emission scanning electron microscope fitted with OXFORD INSTRUMENTS EDS X-Max Aztec software for elemental analysis.

Table 5. Parameters of the manufacturing process of sintered composites with zeolite particles

Tabela 5. Parametry wytwarzania kompozytów zawierających cząstki zeolitu

Material	Compaction pressure	Sintering temperature	Sintering time	Sintering atmosphere
Cu+zeolite	620 MPa	900°C	60 minutes	dissociated ammonia

RESULTS

Microstructural characteristics

The introduction of powdered zeolite causes a distinct change in the microstructure of obtained composites. Zeolite particles of various sizes are very clear in the copper matrix. Differences in a particle size result from the range of the size of the introduced zeolite powder (< 0.2 mm). Mixing the powders of copper and zeolite led to an even distribution of the particles in the matrix.

In certain areas of composites, the zeolite particles are bonded into longitudinal agglomerates. Large clusters of zeolite particles were not observed. Introduced zeolite particles have not dissolved in the matrix in the sintering process, which is associated with high thermal resistance of zeolite particles. There was no diffusion of the elements found in zeolite into the copper matrix. This is important due to the required purity of copper (matrix) and its electrical conductivity. The microstructures of fabricated materials are shown in **Figure 6**.

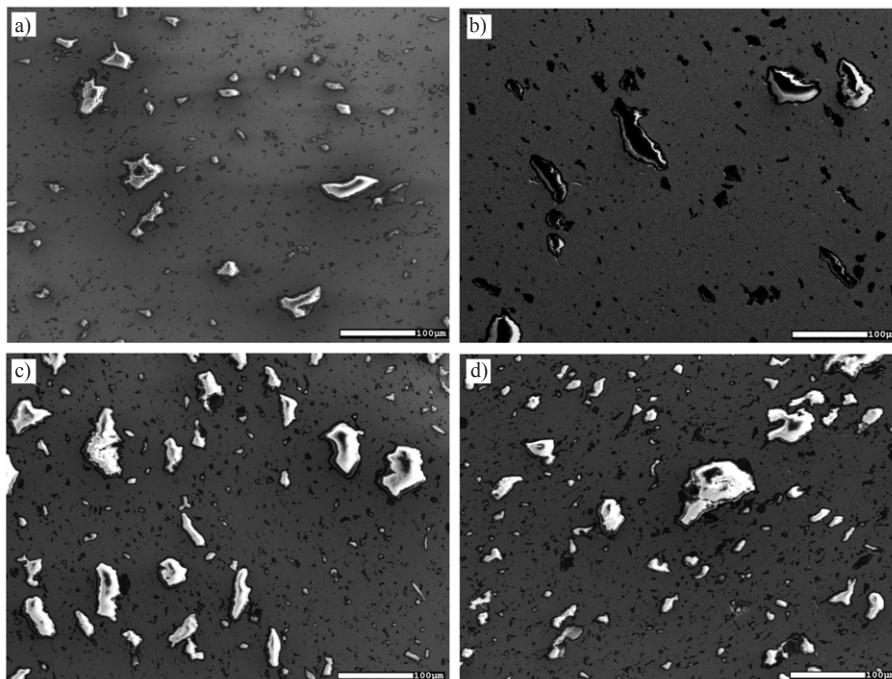


Fig. 6. Microstructures of the sintered compacts observed with a SEM obtained for a) Cu+2.5% zeolite, b) Cu+ 5% zeolite, c) Cu+7.5% zeolite, d) Cu+10% zeolite

Rys. 6. Mikrostruktury spiekanych kompozytów przy SEM uzyskanych dla a) Cu+2,5% zeolitu, b) Cu+5% zeolitu, c) Cu+7,5% zeolitu, d) Cu+10% zeolitu

An example of the distribution of elements in a composite containing 10% zeolite is shown in **Figure 7**. From the mapping, it is clear that the composite contains

only copper, silicon, oxygen, aluminium, potassium, calcium, and iron.

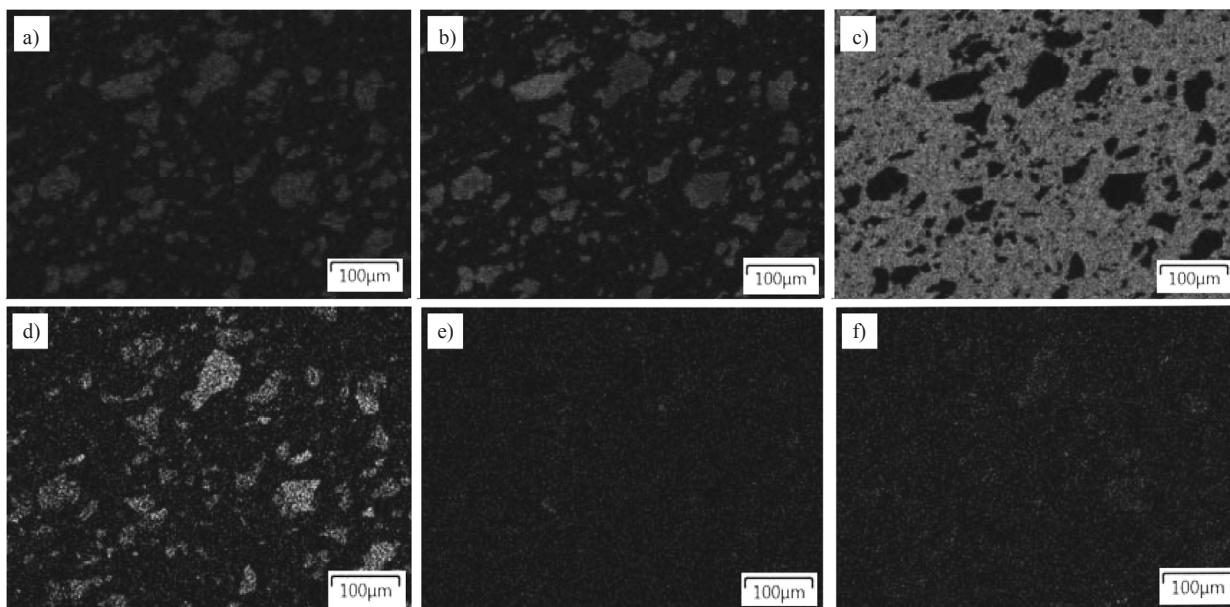


Fig. 7. Distribution of elements in the micro-area of the composite containing 10% zeolite: a) oxygen, b) silicon, c) copper, d) aluminium, e) potassium, f) calcium

Rys. 7. Rozkład pierwiastków w mikroobszarze kompozytu zawierającego 10% zeolitu: a) tlen, b) krzem, c) miedź, d) glin, e) potas, f) wapń

Density and hardness measurements

The results of density and hardness measurements are presented in **Table 6**.

Table 6. Results of the density and hardness measurements

Tabela 6. Wyniki badań gęstości i twardości

Material	Density (g/cm ³)	Relative density (%)	HB
Cu	8.19 ±0.02	92.01	36.65 ±1.5
Cu + 2.5 % zeolite	7.87 ±0.04	89.93	39.42 ±1.8
Cu + 5 % zeolite	7.14 ±0.05	84.51	41.91 ±1.3
Cu + 7.5 % zeolite	6.94 ±0.03	80.76	46.53 ±1.7
Cu + 10 % zeolite	6.53 ±0.07	78.74	48.59 ±1.8

The examination showed that the introduction of zeolite particles into the copper matrix increases the hardness of the composites while reducing the density. The highest hardness was obtained for the composite containing 10% of zeolite particles, which amounted to 48 HB (33% higher than composite made of pure copper). The same phenomenon was also noticed by other researchers [L. 4, 16, 20–23]. The highest density of material was obtained for a composite made from pure copper, which amounted 8.19 g/cm³. The addition of 10% of zeolite caused decrease in density to 6.53 g/cm³.

Electrical conductivity test

The results of electrical conductivity measurements are presented in **Figure 8**.

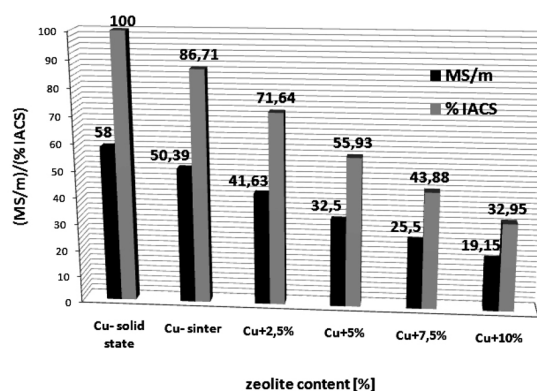


Fig. 8. The results of the electrical conductivity measurements of the copper-zeolite composites

Rys. 8. Wyniki badania przewodności elektrycznej kompozytów Cu-zeolitu

The examination showed that the introduction of zeolite particles into copper matrix caused a decrease in electrical conductivity. This phenomenon is caused by the fact that even a small amount of alloy additives in copper causes a reduction of their electrical conductivity. The highest electrical conductivity was obtained for a composite made of copper powder, which amounted to 50.39 MS/m (14% less than copper in a solid state). The addition of 2.5% of zeolite caused a decrease in electrical conductivity to 41.63 MS/m, but the addition of 10% of zeolite caused a decrease in electrical conductivity to 19.15 MS/m. Similar results were received by other researchers [L. 1, 10, 20–21].

Wear characterization

Weight loss of composites after tribological tests are shown in the **Figure 9**.

Tribological tests have shown that the addition of zeolite particles in an amount of up to 7.5% worsens the abrasion resistance of the composite. A smallest weight loss was observed for the composite containing 10% of zeolite. For the composite containing 10% zeolite, the

weight loss was three times smaller compared to the sample made of pure copper.

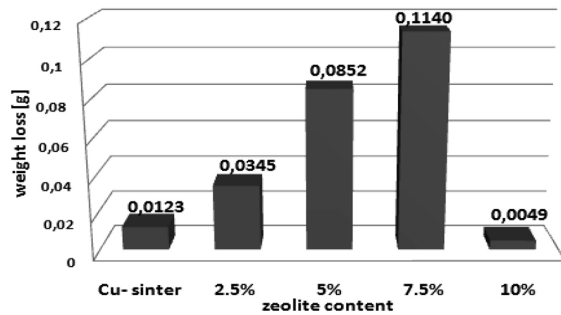


Fig. 9. Weight loss of composites depending on the content of zeolite

Rys. 9. Ubytek masy kompozytów w zależności od zawartości zeolitu

The geometric structures of composites with various amounts of zeolite after tribological tests are showed in **Figures 10–14**.

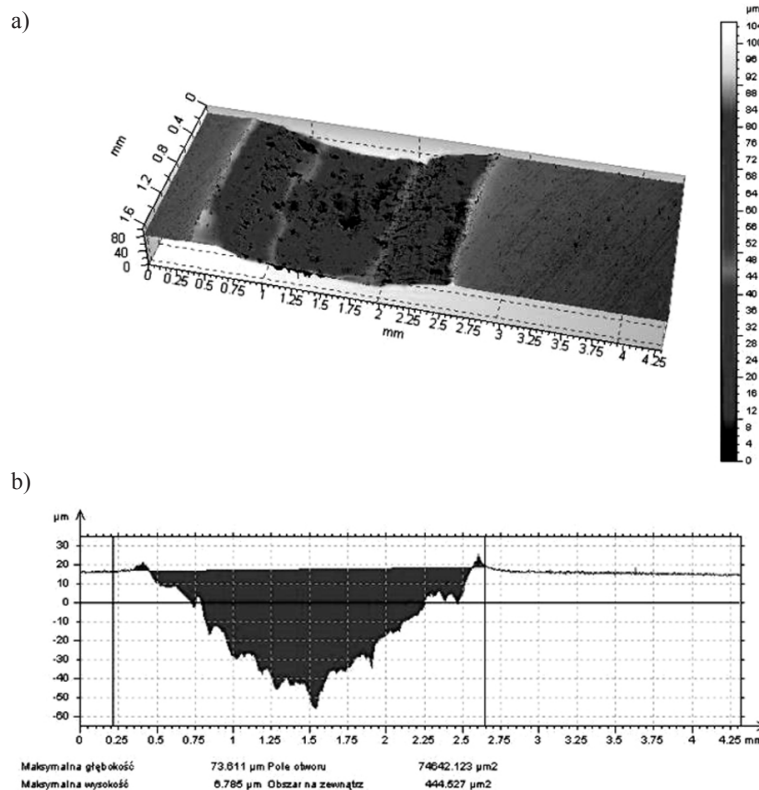


Fig. 10. Surface texture topography of composite made of pure copper after tribological tests under technically dry friction: a) isometric image, b) surface profile

Rys. 10. Struktura geometryczna powierzchni kompozytu wykonanego z czystej miedzi po testach tribologicznych podczas tarcia technicznie suchego: a) obraz izometryczny, b) profil powierzchni

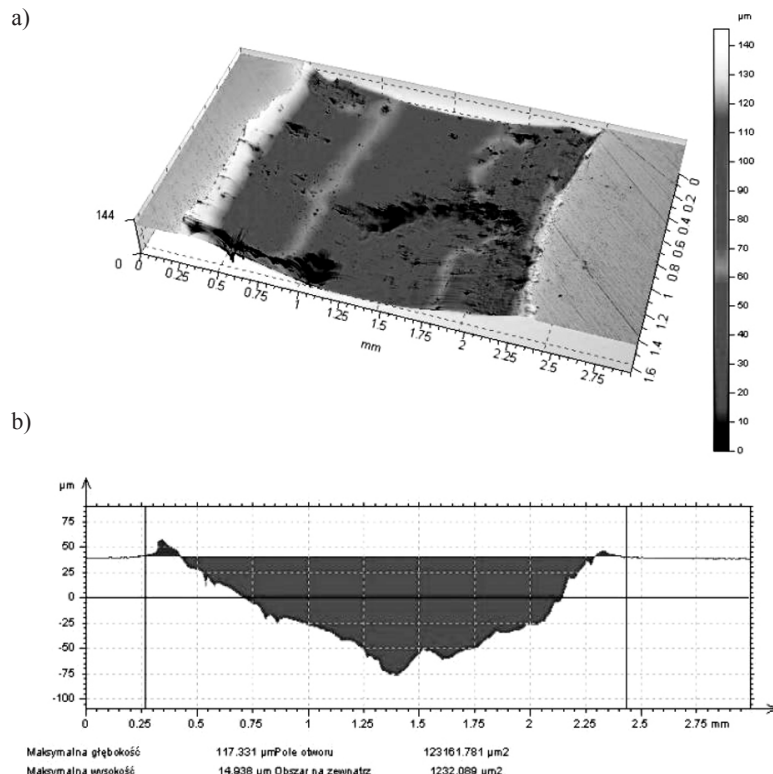


Fig. 11. Surface texture topography of composite containing 2.5% zeolite after tribological tests under technically dry friction: a) isometric image, b) surface profile

Rys. 11. Struktura geometryczna powierzchni kompozytu zawierającego 2,5% zeolitu po testach tribologicznych podczas tarcia technicznie suchego: a) obraz izometryczny, b) profil powierzchni

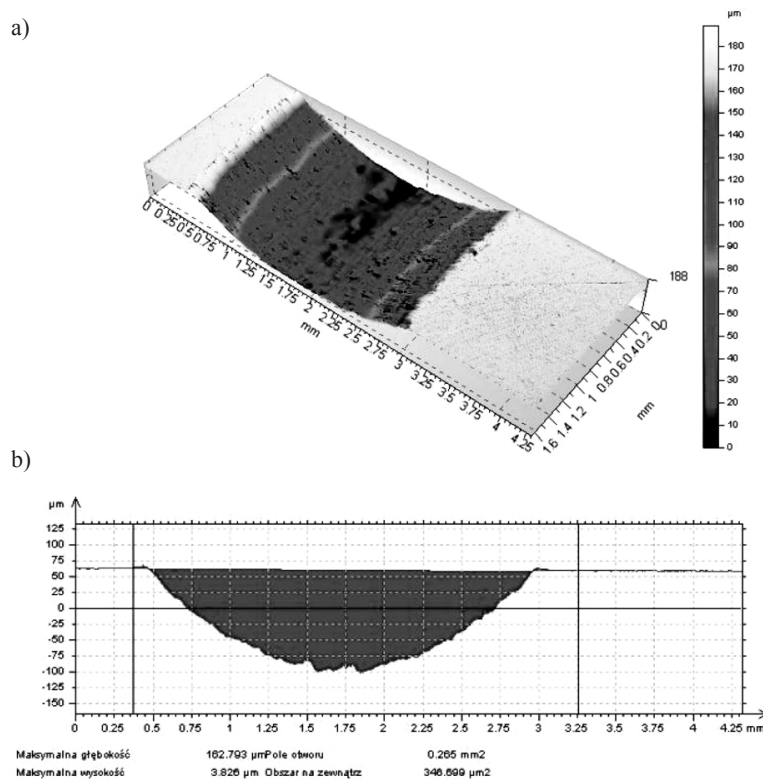


Fig. 12. Surface texture topography of composite containing 5% zeolite after tribological tests under technically dry friction: a) isometric image, b) surface profile

Rys. 12. Struktura geometryczna powierzchni kompozytu zawierającego 5% zeolitu po testach tribologicznych podczas tarcia technicznie suchego: a) obraz izometryczny, b) profil powierzchni

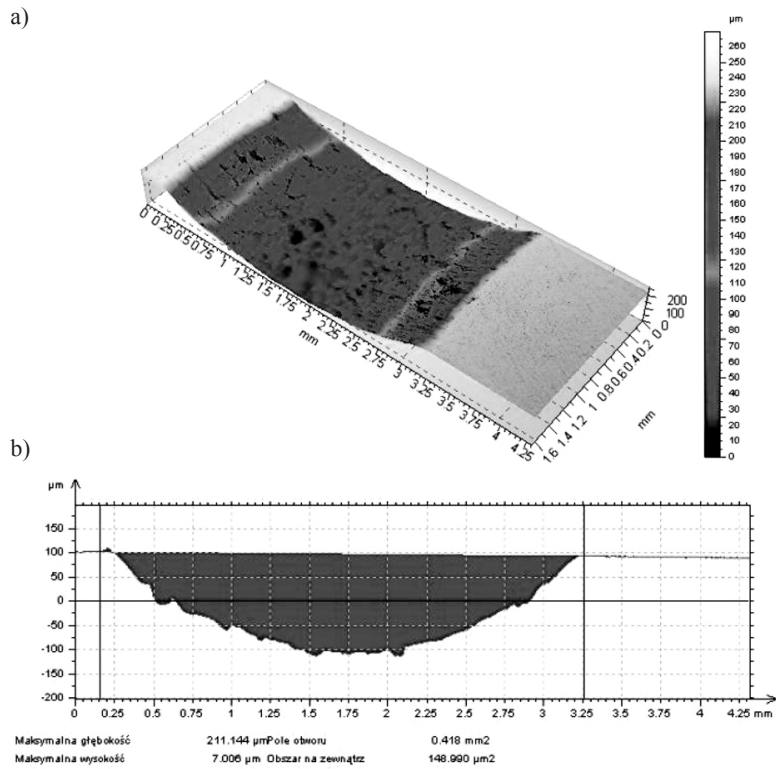


Fig. 13. Surface texture topography of composite containing 7.5% zeolite after tribological tests under technically dry friction: a) isometric image, b) surface profile

Rys. 13. Struktura geometryczna powierzchni kompozytu zawierającego 7,5% zeolitu po testach tribologicznych podczas tarcia technicznie suchego: a) obraz izometryczny, b) profil powierzchni

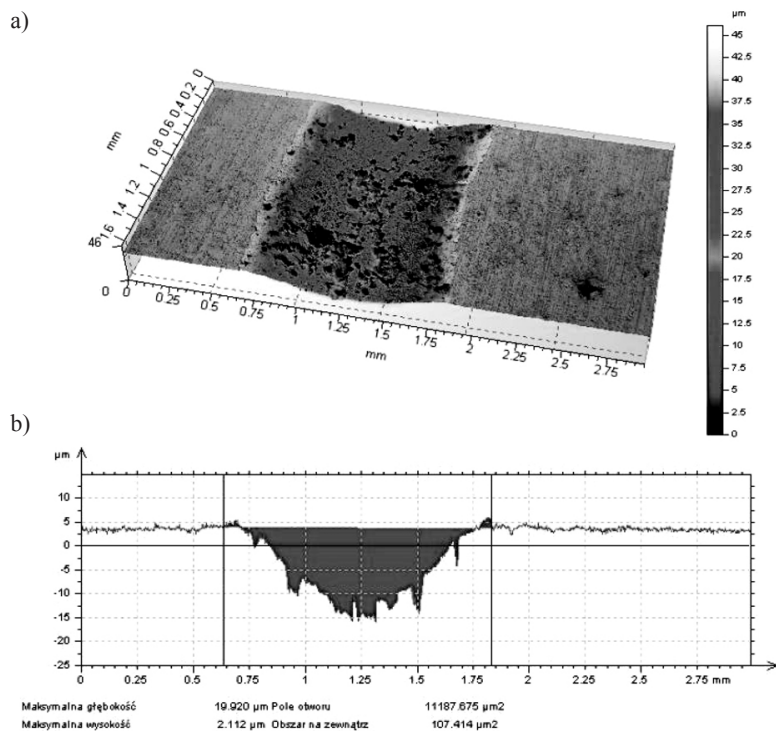


Fig. 14. Surface texture topography of composite containing 10% zeolite after tribological tests under technically dry friction: a) isometric image, b) surface profile

Rys. 14. Struktura geometryczna powierzchni kompozytu zawierającego 10% zeolitu po testach tribologicznych podczas tarcia technicznie suchego: a) obraz izometryczny, b) profil powierzchni

The analysis of the geometric structure of the surface showed that the smallest material consumption was obtained for a composite containing 10% zeolite. Thus, the results of the weight loss tests were confirmed. In **Figures 11–13** in places of abrasion marks, there are numerous irregular hollows created as a result of pulling out of zeolite particles during the tests, which may cause an increased loss of the weight of composites containing up to 7.5% zeolite.

CONCLUSIONS

The analysis of the microstructure of the composites showed that the zeolite powder particles combine into agglomerates. Before sintering, powders should be mixed thoroughly to break up the agglomerates and obtain a homogeneous mixture. The sintering parameters were chosen correctly. The microstructural examinations showed that there were no discontinuities at the interface between the matrix and the ceramic particles. A very

good bonding of zeolite particles with the copper matrix was obtained, without voids, only the pores occurring in sintered metals were visible on the micrographs. Zeolite particles were clearly visible in the form of irregular precipitates. The introduction of zeolite particles resulted in an increase in the hardness of the composites and a decrease in the density and electrical conductivity. Tribological tests have shown that the introduction of 10% zeolite particles increases abrasion resistance. In the case of sinters containing up to 7.5% zeolite, a larger loss of weight was observed than for the composite made of copper powder. This may be due to the introduction of large size of zeolite particles (less than 200 μm), which have been pulling out from the matrix during the test, or as a result of the combining the particles into agglomerates. Confirmation of the aforementioned assumptions requires additional tests. The composite containing 10% zeolite has properties qualifying it for use as a material for electric brushes (satisfactory electrical conductivity and abrasion resistance).

REFERENCES

1. Lee D.W., Kim B.K.: Nanostructured Cu-Al₂O₃ composite produced by thermochemical process for electrode application. *Materials Letters*, 2004, vol. 58, pp. 378–383.
2. Shi Z., Yan M.: The preparation of Al₂O₃-Cu composite by internal oxidation. *Applied Surface Science*, 1998, vol. 134, pp. 103–106.
3. Kruger C., Mortensen A.: In situ copper–alumina composites. *Materials Science and Engineering A*, 2013, vol. 585, pp. 396–407.
4. Dash K., Ray B.C., Chandra D.: Synthesis and characterization of copper–alumina metal matrix composite by conventional and spark plasma sintering. *Journal of Alloys and Compounds*, 2012, vol. 516, pp. 78–84.
5. Rajkovic V., Bozic D., Devecerski A., Jovanovic M.T.: Characteristics of copper matrix simultaneously reinforced with nano- and micro-sized Al₂O₃ particles. *Materials Characterization*, 2012, vol. 67, pp. 129–137.
6. Konieczny M.: Mechanical properties of Ti-(Al₃Ti+Al) and Ti-Al₃Ti laminated composites, *Composites Theory and Practice*, vol. 13, 2013, pp. 102–106.
7. Mola R., Konieczny M.: Spiekane kompozyty uzyskane z proszku miedzi, tytanu i aluminium, *Rudy i metale niezelazne*, vol. 54, 2009, pp. 26–30.
8. Wang C., Lin H., Zhang Z., Li W.: Fabrication, interfacial characteristics and strengthening mechanism of ZrB₂ microparticles reinforced Cu composites prepared by hot-pressed sintering, *Journal of Alloys and Compounds*, vol. 748, 2018, pp. 546–552.
9. Li J.F., Chen B., Tang H., Zhang S., Li C.: Tribological behavior of Cu- based composites with NbSe₂ and TiB₂, *Digest Journal of Nanomaterials and Biostructures*, vol. 12, No. 4, 2017, p. 1205–1214.
10. Taha M.A., Zawrah M.F.: Effect of nano ZrO₂ on strengthening and electrical properties of Cu- matrix nanocomposites prepared by mechanical alloying. *Ceramics International*, 2017, vol. 43, pp. 12698–12704.
11. Samal C.P., Parihar J.S., Chandra D.: The effect of milling and sintering techniques on mechanical properties of Cu-graphite metal matrix composite prepared by powder metallurgy route, *Journal of Alloys and Compounds*, vol.569, 2013, pp. 95–101.
12. Fathy A., Elkady O., Abu-Oqail A.: Synthesis and characterization of Cu-ZrO₂ nanocomposite produced by thermochemical process. *Journal of Alloys and Compounds*, 2017, vol. 719, pp. 411–419.
13. Fathy A.: Investigation on microstructure and properties of Cu-ZrO₂ nanocomposites synthesized by in situ processing, *Materials Letters*, vol. 213, 2018, pp. 95–99.
14. Shojaeepour F., Abachi P., Purazrang K., Moghani A.H.: Production and properties of Cu/Cr₂O₃ nanocomposites. *Powder Technology*, 2012, vol. 222, pp. 80–84.

15. Rahimian M., Parvin N., Ehsani N.: Investigation of particle size and amount of alumina on microstructure and mechanical properties of Al matrix composite made by powder metallurgy, *Materials Science and Engineering A*, vol. 527, 2010, pp. 1031–1038.
16. Konieczny M.: The effect of sintering temperature, sintering time and reinforcement particle size on properties of Al_2O_3 composites. *Composites Theory and Practice*, 2012, vol. 12, no. 1, pp. 39–43.
17. Kaczmar J.W., Pietrzak K., Włosiński W.: The production and application of metal matrix composite materials. *Journal of Materials Processing Technology*, 2000, vol. 106, pp. 58–67.
18. Rajkovic V., Bozic D., Stasic J., Wang H., Jovanovic M.T.: Processing, characterization and properties of copper-based composites strengthened by low amount of alumina particles, *Powder Technology*, vol. 268, 2014, pp. 392–400.
19. Łach M., Mięka J., Hebda M.: Thermal analysis of the by-products of waste combustion, *Journal of Thermal Analysis and Calorimetry* Vol. 125, Issue 3, pp. 1035–1045.
20. Mięka J., Łach M., Kowalski J.S.: Copper Matrix Composites Reinforced with Volcanic Tuff, *Metalurgija* Vol. 54, 2015, pp. 143–146.
21. Łach M.: Structure of metal matrix composites with an addition of tuff. *Archives of Foundry Engineering*, 2010, vol. 10, Special Issue 3, pp. 135–140.
22. Borowiecka-Jamrozek J., Depczyński W.: The effect of the addition of zeolite on the properties of a sintered copper-matrix composite. In *METAL 2017: 26rd International Conference on Metallurgy and Materials*. Ostrava: TANGER, 2017, pp. 1652–1657.
23. Cichiszewski G.W., Andronikaszewski G.N., Kuroń Ł.D.: *Zeolity naturalne*, WNT, Warszawa 1990.
24. Gottardi G., Galli E.: *Natural Zeolites, Mineral and Rocks* 18, Springer-Verlag, Berlin Heidelberg 1985, pp. 256–284.
25. Nanbin H., Dianyue G., Bekkum H., Flanigen E., Jacobs P., Jansen J.: *Introduction to Zeolite Science and Practice*. No 137, 2nd Completely revised and expanded edition, Elsevier, New York 2001, pp. 54–59.
26. Turel A., Slavic J., Boltezar M.: Electrical contact resistance and wear of a dynamically excited metal-graphite brush, *Advances in Mechanical Engineering*, vol. 9(3), 2017, pp. 1–8.